Available online at www.sciencedirect.com
SCIENCE DIRECT
Comparative Biochemistry and Physiology, Part B 143 (2006) 37 – 43
CBP
www.elsevier.com/locate/cbpb

Dromedary glycosaminoglycans: Molecular characterization of camel lung and liver heparan sulfate

Mohammad Warda [a], Robert J. Linhardt [b,*]

[a] Department of Biochemistry, Faculty of Veterinary Medicine, Cairo University, Egypt
[b] Department of Chemistry and Chemical Biology, Biology and Chemical and Biological Engineering, Rensselaer Polytechnic Institute, Troy, NY 12180, USA

Received 10 June 2005; received in revised form 27 September 2005; accepted 28 September 2005
Available online 17 November 2005

Abstract

Glycosaminoglycans (GAGs) are the portion of a proteoglycan that determine its final shape and function. The molecular structure of predominant GAG species in camel liver and lung is reported for the first time. The one-humped camel survives in an extreme, arid habitat and, thus, offers a good model to study the role of glycomics on homeostasis. Heparan sulfate (HS) from the lung and liver of the one-humped camel were isolated. Characterization of these newly isolated glycosaminoglycans included ^{1}H NMR spectroscopy and disaccharide compositional analysis. The relative molecular weight of these GAGs was estimated by gradient polyacrylamide gel electrophoresis and their degree of sulfation was also assessed. Anticoagulant activity was determined using an anti-factor Xa assay and the HS from camel lung shows ~50% of heparin's activity. The structural differences of camel liver GAGs compared to human and porcine liver heparin and HS is discussed. Camel lung heparan sulfate resembles both heparin and HS in its structure and properties suggesting that it is either a highly sulfated form of HS, a mixture of heparin and HS or an undersulfated heparin.

Keywords: Heparin; Heparan sulfate; Glycosaminoglycans; One-humped camel; Mammalian; Liver; Lung; Disaccharide; Anticoagulant; Factor Xa

1. Introduction

The biological interactions mediated by proteoglycans (PGs) are believed to be due primarily to the presence of glycosaminoglycan (GAG) chains (Nakato and Kimata, 2002; Capila and Linhardt, 2002). Since the PGs are often localized on cell surfaces and in the extracellular matrix, they have important function in cell–cell interaction, binding a variety of proteins and localizing these at the cell surface (Hardingham and Fosang, 1992). Heparin and heparan sulfate (HS) GAGs bind over 100 different proteins, including enzymes, protease inhibitors, lipoproteins, growth factors, chemokines, selectins, extracellular matrix proteins, receptor proteins, viral coat proteins and nuclear proteins (Linhardt and Toida, 2004; Capila and Linhardt, 2002). Heparin and HS are closely related, overlapping structures that are widely distributed in invertebrates (Medeiros et al., 2000; Nobuo, 2003; Cesaretti et al., 2004), as well as in vertebrates (Gomes and Dietrich, 1982). Moreover, HS GAGs modulate many biological activities including signal transduction (Ibrahimi et al., 2005), inflammation (Peterson et al., 2004), complement activation (Yu et al., 2005) and cAMP-dependent substrate phosphorylation catalyzed by protein kinase (Dittmann et al., 1998). Some of the biological roles of GAGs have been exploited for the design and preparation of therapeutic drugs. Heparin, a highly sulfated HS GAG, for example, is widely used as a clinical anticoagulant (Linhardt, 2003). A number of growth factors, including members of the fibroblast growth factor (FGF) family, hepatocyte growth factor, vascular endothelial growth factor and heparin-binding epidermal growth factor, are dependent on HS for biological activity mediated through their high-affinity signal-transducing receptors (Ibrahimi et al., 2005). Thus, it is important to have a detailed understanding of heparin/HS structure to develop structure activity relationships. Much research has been performed to determine the structure of heparin/HS isolated different species and tissues (Gomes and Dietrich, 1982; Medeiros et al., 2000; Nobuo,

Abbreviations: GAG, glycosaminoglycans; HS, heparan sulfate; PG, proteoglycan.

* Corresponding author. Tel.: +1 518 276 3404; fax: +1 518 276 3405.

1096-4959/$ - see front matter © 2005 Published by Elsevier Inc.
doi:10.1016/j.cbpb.2005.09.015

2003; Cesaretti et al., 2004). Despite these efforts, there still remains the question about how the fine structure of the GAG moiety of these HSPGs regulates their biological functions. In the present study, we examine the fine molecular structure of GAGs isolated from the camel. This unique creature resides in harsh arid environments. Thus, such a study might reveal peculiarities in the GAG structure that relate to this environment. Compared to many other mammals, the camel has offered a unique model of altered membrane phospholipids structure (Warda and Zeisig, 2000), GAG structure (Warda et al., 2003), protein–protein interaction (Dumoulin et al., 2002), and genetic makeup (Warda et al., submitted for publication).

The camel has very characteristic hepatic tissues with well-developed connective tissue septa (Lalla and Drommer, 1997) that resemble, to a great extent, fibrosed liver in other mammals. PGs participate in fibrogenesis. The majority of liver-specific HSPGs, such as syndecan-1 and fibroglycan, are produced by hepatocytes. The extracellular matrix HSPG perlecan is synthesized by non-parenchymal liver cells. The amount of perlecan is very low in normal liver, but increases dramatically in liver fibrosis (Kovalszky et al., 1988). Liver is also a target for a number of pathogens and liver HS has been demonstrated in several cases to play a pivotal role in infectivity (Chen et al., 1997; Rathore et al., 2001; Barth et al., 2003). Liver HSPGs at the endothelial level act as critical receptors for apoE and is involved in lipid metabolism (Bocksch et al., 2001; Dong et al., 2001; Bazin et al., 2002).

Camelids have a characteristic low hematocrit and a small red blood cell volume (Warda and Zeisig, 2000). The saturation of blood with oxygen in the lung is favored by a high blood oxygen affinity, oxygen supply being facilitated by low diffusion distances in tissue. Loading, as well as unloading, of oxygen is improved by a relatively high oxygen transfer conductance of the red blood cells, which is due to their small size compensating for their low hematocrit (Jurgens et al., 1988). Thus, understanding the structure of camel lung GAGs might improve our understanding of homeostasis regulation in an arid environment. Finally, the appearance of bovine spongiform encephalopathy, “mad cow disease”, and its apparent link to the similar prion-based Creutzfeldt–Jakob disease in humans (Schonberger, 1998), has recently opened the prospect of importance of deriving GAGs for therapeutic uses from the liver and lung of the camel (Warda et al., 2003).

2. Materials and methods

2.1. Materials

Chondroitin ABC lyase from *Proteus vulgaris*, endonuclease (EC 3.1.30.2) from *Serratia marcescens* and heparin lyase I (heparinase EC 4.2.2.7), heparin lyase II (heparitinase II), heparin lyase III (heparitinase I EC 4.2.2.8) from *Flavobacterium heparinum* and Dowex macroporous resin as strong basic anion exchanger (SAX) were purchased from Sigma Chemical Co. (St. Louis, MO, USA). Spectra/Por® dialysis tubing MWCO 3500 was from Spectrum Medical Industries, Inc. (Los Angeles, CA, USA). Standard heparins obtained from porcine intestine were purchased from Celsus Laboratories Inc. (Cincinnati, OH, USA). Heparin assay kit used for the quantitative determination of heparin was purchased from Sigma Diagnostics (St. Louis, MO, USA). Actinase E (EC 4.2.2.6) was a gift from the graduate school of pharmaceutical science, Chiba University, Japan. All other reagents used were analytical grade.

2.2. Preparation of liver and lung GAGs

Fresh liver and lung tissues of one dromedary camel (*Camelus dromedarius*) were collected shortly after animal slaughter and treated as previously described (Warda et al., 2003). Briefly, fresh samples of camel liver or lung (50 g) were cut into small pieces and homogenized in a blender. The homogenate was digested by actinase E (10 mg/g) using 0.05 M Tris–acetate buffer (pH 8.0) at 50 °C for 12 h. The actinase-treated homogenate was boiled in water bath for 30 min to deactivate the protease, centrifuged (1500×*g*) at 4 °C for 30 min. The recovered supernatant was added to a pre-activated (washed extensively with methanol, H_2O, 2 M NaCl, H_2O) SAX Dowex macroporous resin that equilibrated with 0.1 M NaCl. The resin was washed with water followed by 3 wt.% NaCl to elute residual peptides and low molecular weight contaminants. The resin was then eluted by 16 wt.% NaCl. The GAGs eluted from the SAX resin were precipitated by addition of methanol 80 vol.% (v/v). The precipitated material was recovered by centrifugation and dialyzed in cellulose membrane tubing (MW cutoff 3500) against deionized water overnight at 4 °C and freeze-dried. The crude liver and lung GAGs of camel (20 mg/mL) were treated with chondroitin lyase ABC (0.5 unit/100 mg in 50 mM sodium acetate, pH 8) at 37 °C for 24 h in sealed tubes. After digestion, the reactions were terminated by heating in a boiling water bath for 5 min, and the digested samples were desalted using microanalysis desalting spin column (Amika Corp®) and freeze-dried. The dried material was then re-suspended in 20 mM Tris–HCl buffer (pH 8) containing 2 mM magnesium chloride and digested with endonuclease (2500 units/g) for 12 h at 37 °C (Warda et al., 2003). After endonuclease digestion, NaCl concentration was brought to 16 wt.% and the GAGs were precipitated by adding methanol to 80 vol.%. The recovered precipitate was dissolved in 10 mL of de-ionized water and dialyzed overnight at 4 °C and the retentate was freeze-dried. The dried GAG was then subjected for structural and functional characterization.

2.3. Chemical characterization

Azure A assay was performed to estimate the level of sulfo group substitution of the purified GAGs. Metachromasia of the blue dye on addition of negatively charged GAGs results in a concentration-dependent increase in absorbance at 530 nm (Grant et al., 1984). Carbazole assay was performed to determine content of uronic acid in the GAG preparation by determining the absorbance at 525 nm (Bitter and Muir, 1962).

Porcine intestinal heparin standard was used in both cases to prepare standard curves.

2.4. ^1H NMR analysis

NMR spectroscopy was performed on samples (~5 mg) dissolved in D_2O (99.96 at.%), filtered through a 0.45 μm syringe filter, freeze-dried twice from D_2O to remove exchangeable protons. One-dimensional (1D) was performed on a Bruker DRX-600 equipped with NMR processing and plotting software.

2.5. Enzymatic depolymerization of glycosaminoglycans

For enzymatic depolymerization, the previously chondroitin ABC lyase-digested samples were next digested in heparinase lyase I, II, III (Griffin et al., 1995). Dried samples were dissolved in buffer (50 mM sodium phosphate buffer, pH 7.1 and 100 mM NaCl) at a concentration of 10 mg/mL. Each heparin lyase was added at 0, 8 and 16 h to a final concentration of 0.02 mU/mg GAG dry mass. The reaction was performed in sealed tubes at 37 °C over 36 h. The efficiency of GAGs depolymerization was monitored by measuring the increase of absorbance at 232 nm. Standard porcine heparin and heparan sulfates were treated in a similar manner to serve as controls. The reaction was boiled, desalted and freeze-dried as previously described in chondroitin lyase ABC digestion step.

2.5.1. Gradient polyacrylamide gel electrophoresis

The average molecular masses of crude liver and lung GAGs were analyzed by polyacrylamide linear gradient resolving gels (14 × 28 cm, 12–22% acrylamide) prepared and run as described previously (Toida et al., 1997). The average molecular mass of isolated GAGs was determined by comparing with banding ladder of heparin oligosaccharide standards prepared from bovine lung heparin and tetrasaccharide marker was added to identify the bands (UN-Scan – IT gel, automated digitizing system, version 4.3 for Macintosh, Silk Scientific, CA, USA).

2.5.2. Determination of unsaturated disaccharides from camel liver and lung heparin/HS GAGs

Unsaturated disaccharides produced enzymatically from GAGs were determined by reversed-phase ion-pairing (RPIP) high-performance liquid chromatography (HPLC) with UV detection (Thanawiroon and Linhardt, 2003). The separation of samples (5 μl each) was done on Discovery C-18 column (5 μm, 4.6 × 250 mm^2, Supelco®). The system included Shimadzu LC-10AI pumps and a Shimadzu SPD-10Ai UV/Visible detector. Unsaturated disaccharides were eluted by isocratic elution with flow rate of 1 mL/min elution mixture was formed from 15 mM tributylamine, 50 mM ammonium acetate and 15 mm acetic acid in acetonitrile/water (20:80, v:v). A mixture of 8 available unsaturated disaccharides of different sulfation pattern (Sigma) was used to detect the time of elution of each unsaturated disaccharide. Disaccharides signals were detected at 232 nm. The data acquisition and processing were performed using CLASS vp 4.2 software (Shimadzu Corp., Japan).

2.5.3. Anticoagulant activity assay

Factor Xa inactivation was used to assess the anticoagulant activity of GAGs prepared from camel liver and lung using a Heparin Assay Kit (Sigma). Factor Xa and antithrombin III are both present in excess; the inhibition of factor Xa is directly proportional to the limiting concentration of heparin. Thus, residual factor Xa activity, measured with factor Xa-specific chromogenic substrate, is inversely proportional to the heparin concentration (Teien et al., 1976; Teien and Lei, 1977).

3. Results and discussion

The recovery of camel liver heparin/HS GAGs was 180 mg/kg fresh wet mass and the recovery camel lung heparin/HS was 320 mg/kg mass of fresh wet mass. The average recovery of the camel heparin/HS GAGs from these two organs was much higher than that reported in our previous studies on human liver heparin/HS (Vongchan et al., 2005) but lower than reported for camel intestinal heparin/HS (Warda et al., 2003). The average molecular mass of isolated heparin/HS GAGs were determined by polyacrylamide gel electrophoresis from the broad band associated with isolated GAGs (Fig. 1). The camel liver and lung heparin/HS GAGs both had an average molecular mass of ~21 kDa. The camel-derived heparin/HS GAGs were more polydisperse than porcine intestinal heparin and had nearly

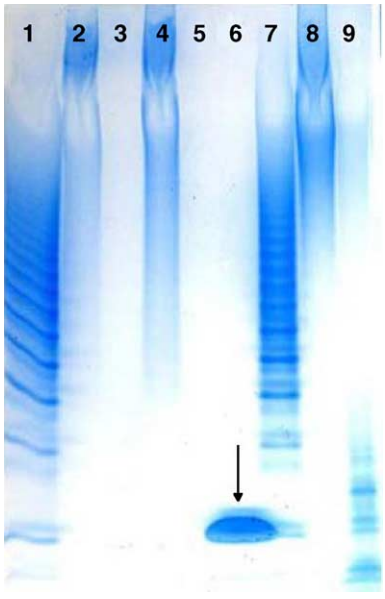

Fig. 1. Alcian blue-stained gradient polyacrylamide gel containing liver and lung and porcine intestinal GAGs. Lanes 1 and 7: heparin-derived oligosaccharide standards enzymatically prepared from bovine lung heparin (Edens et al., 1992); lane 2: GAGs of camel liver; lane 3: heparin lyases-treated camel liver GAGs; lane 4: GAGs of camel lung; lane 5: heparin lyases-treated camel lung GAGs; lane 6: heparin hexasulfated tetrasaccharide standard indicated by the arrow (Pervin et al., 1995); lane 8: standard porcine intestinal heparin; lane 9: treatment of standard porcine intestinal heparin with heparin lyases.

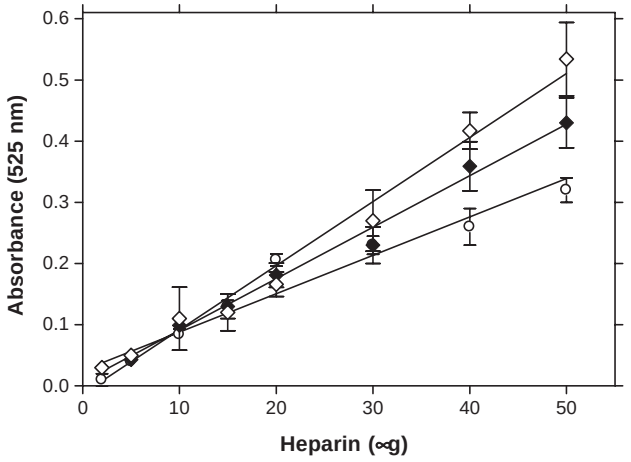

Fig. 2. Carbazole assay of camel lung (♦) and liver (○) crude GAGs compared with standard porcine intestinal heparin (◇).

twice the average molecular mass of porcine intestinal heparin. The complete conversion of GAG to oligosaccharide on treatment with heparin lyases (Fig. 1, lanes 3 and 5) confirmed that contaminating nucleic acids and chondroitin and dermatan sulfate GAGs had been successfully removed by the chondroitinase and endonuclease treatment used in the purification process. Carbazole assay was next used to determine the uronic acid component of glycosaminoglycan (Fig. 2). Standard porcine intestinal (pharmaceutical) heparin determined by carbazole assay gave a line with equation $y=0.01x-0.013$, $r^2=0.98$, showing a 20% higher slope, and hence higher concentration of glucuronic and iduronic acid per unit mass, than did camel lung heparin/HS GAGs that had a line equation $y=0.008x-0.01$, $r^2=0.99$. Camel liver heparin/HS GAGs, however, gave a line equation $y=0.006x-02$, $r^2=0.94$ with 40% reduction in glucuronic and iduronic acid concentration per unit mass than that of porcine intestinal heparin. The lower amount of uronic acid for a given mass of GAG can be explained by the presence of non-GAG contaminants, such as residual salt or water, or a higher level of sulfation. Next, the charge density was estimated using Azure A assay. A plot of

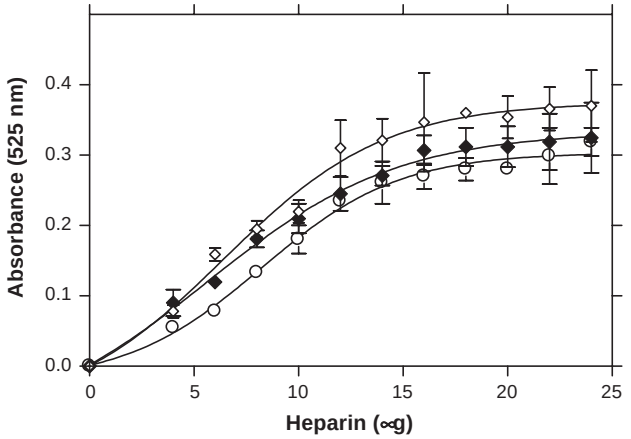

Fig. 3. Azure A assay of camel lung (♦) and liver crude GAGs compared with standard porcine intestinal heparin (◇).

Azure A metachromatic activity as a function of concentration for camel lung GAGs (Fig. 3) showed the normal hyperbolic saturation curve for camel heparin/HS GAGs as well as standard porcine intestinal heparin. The line of equation of

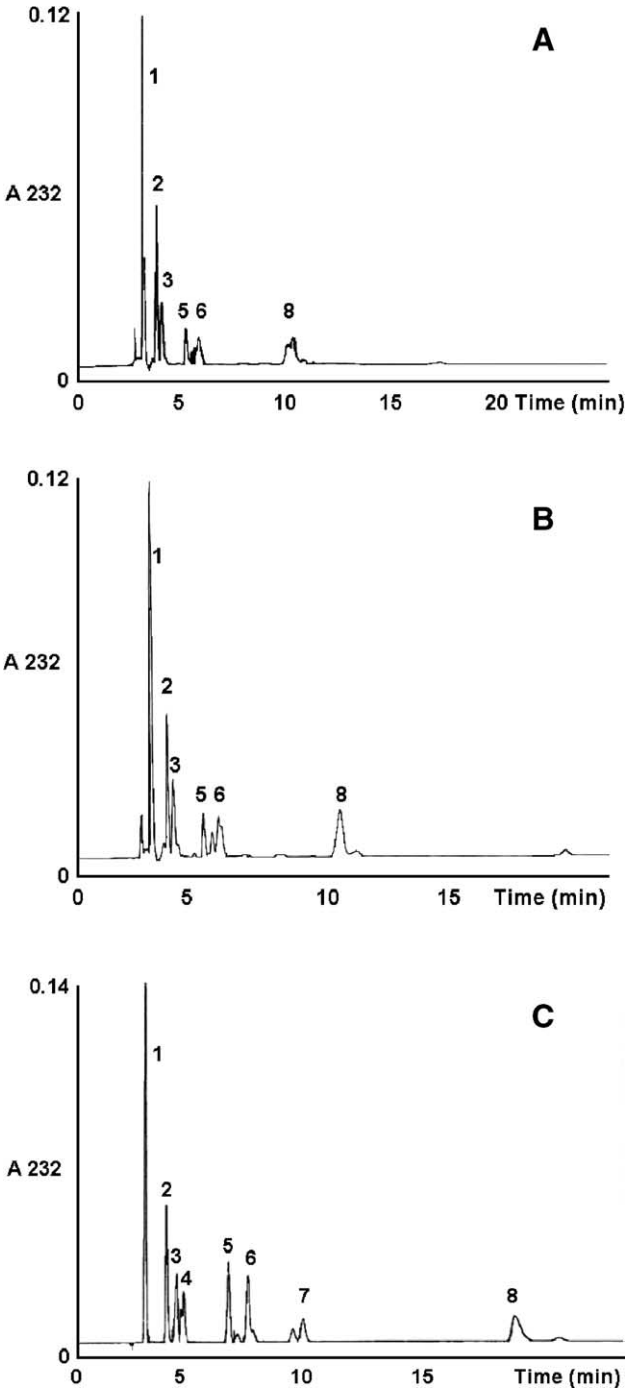

Fig. 4. Unsaturated disaccharide analysis of heparinase-treated camel liver and lung GAGs (A and B) compared to porcine intestinal heparin-derived standard mixture of different unsaturated disaccharides (C) using RPIP HPLC: Peak **1** is ΔUA–GlcNAc, peak **2** ΔUA–GlcNS, peak **3** is ΔUA–GlcNAc6S, peak **4** ΔUA2S–GlcNAc, peak **5** ΔUA–GlcNS6S, peak **6** is ΔUA2S–GlcNS, peak **7** is ΔUA2S–GlcNAc6S, peak **8** is ΔUA2S–GlcNS6S. Analysis was performed on different days so that the retention times vary. Peaks were identified by co-injection with disaccharide standards (Warda et al., 2003).

Table 1
Unsaturated disaccharide proportion (mol%)[a]

	(1) ΔUA–GlcNAc	(2) ΔUA–GlcNS	(3) ΔUA–GlcNAc6S	(4) ΔUA2S–GlcNAc	(5) ΔUA–GlcNS6S	(6) ΔUA2S–GlcNS	(7) ΔUA2S–GlcNAc6S	(8) ΔUA2S–GlcNS6S	Degree of sulfation[b]
Porcine intestine heparin[c]	3.1	3.6	14.5	1.2	24.9	12.4	nd	40.3	2.55
Camel lung HS	9.5	19.2	19.9	nd	7.4	12.6	nd	31.4	1.73
Camel intestine HS[d]	18.4	22.0	20.9	nd	11.4	12.8	nd	14.5	1.35
Human liver HS[d]	37.3	15.5	9.8	1.2	7.8	5.9	0.7	21.8	1.21
Camel liver	19.7	25.9	27.2	nd	9.1	10.8	nd	7.3	1.15
Porcine liver HS[d]	47.9	10.8	10.2	nd	5.6	4.4	nd	21.2	1.05

[a] The numbering of disaccharides **1**–**8** corresponds to those used in Fig. 4 from which the peak areas corresponding to mol% were obtained.
[b] Sulfo groups/disaccharide calculated from disaccharide analysis.
[c] Vongchan et al., 2005.
[d] Warda et al., 2003.

the first half of the curve that explicit linear increase (data below 20 μg heparin) gave a line of equation $y=0.018x+0.02$ with coefficient of determination $r^2=0.98$ for camel lung heparin/HS GAGs, while that of camel liver heparin/HS GAGs gave a line of equation $y=0.017x-0.01$ with coefficient of determination $r^2=0.97$. Pharmaceutical porcine heparin standard gave a line of equation $y=0.02x+0.02$, $r^2=0.97$. The negatively charged groups in heparin/HS GAGs that contribute to protein binding and hence biological activity include carboxyl, *N*- and *O*-sulfo groups. *N*-sulfo groups are located at the C-2 position of the GlcNp residues in heparin (85% *N*-sulfo, 15% *N*-acetyl) and HS (10% *N*-sulfo, 90% *N*-acetyl) (Bazin et al., 2002). Camel liver and camel lung heparin/HS showed ~30% lower density of negative charge per unit mass when compared with porcine intestinal heparin standard.

Since Azure A assay affords only a qualitative or semi-quantitative value of charge density, disaccharide analysis of each heparin (Fig. 4) was used to quantify the negative charges/disaccharide ratio. The disaccharide proportion (mol%) (Table 1) can be used to determine the degree of sulfation (the charge density, or negative charges/disaccharide ratio, is one order of magnitude higher than the degree of sulfation due to the presence of the carboxyl group) of 1.73 and 1.15 for the camel lung and camel liver HS, respectively. The degree of sulfation of camel lung HS is higher than other HS samples yet still considerably lower than that of porcine intestinal heparin. Thus, the relatively high level of sulfation of camel lung GAG might be explained by it being a highly sulfated HS, a mixture of HS and heparin or an undersulfated heparin. Camel lung GAG also contains a considerably higher level of trisulfated disaccharide (ΔUA2S–GlcNS6S) than other HS samples tested. In contrast, the degree of sulfation of camel liver HS is more typical for an HS; it is lower than camel intestinal HS but is between the values observed for porcine and human liver HS. The disaccharide composition of camel liver HS, however, is strikingly different from that of other liver HS samples examined in our laboratory, with low levels of both unsulfated (ΔUA–GlcNAc) and trisulfated (ΔUA2S–GlcNS6S) disaccharides. Of particular note is the exceedingly low level of trisulfated disaccharide, since a octasaccharide sequence comprised of this repeating disaccharide corresponds to the liver receptor for apoE (Dong et al., 2001) as well as a receptor for the circumsporozoite form of the malaria parasite (Rathore et al., 2001). This peculiar structural feature of camel HS may play a role in maintaining the lower level of camel LDL compared to the LDL levels reported in other mammals (Nazifi et al., 2000). Furthermore, unlike many other animal species (Mackenstedt et al., 1989), the camel is not susceptible to many zoonotic diseases, including malaria. These observations appear to be consistent with the unique structural features of camel liver HS.

Proton NMR of both camel liver and camel lung heparin/HS GAGs (Fig. 5) show that both contain a singlet at 2 ppm corresponding to an *N*-acetyl methyl of GlcNAc peak (peak **10**). Both samples contain substantially more GlcNAc than

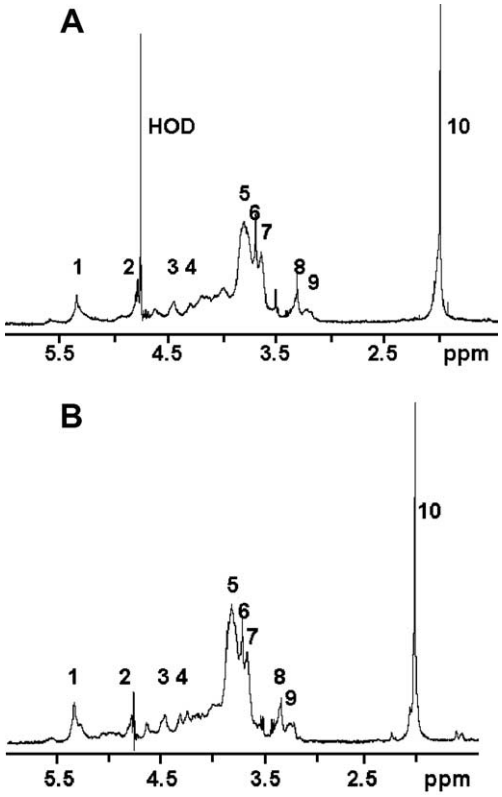

Fig. 5. 1D ^{1}H NMR spectrum of camel liver (A) and lung (B) GAGs. Peaks are designed as follows: **1** GlcNS (H-1) and IdoA2S (H-1), **2** IdoA2S (H-5) (overlapped with HOD signal), **3** GlcA (H-1), **4** IdoA2S (H-2), **5** GlcNAc (H-6), **6** GlcA (H-4, H-5), **7** GlcA (H-3), **8** GlcA (H-2), **9** GlcNS (H-2), **10** *N*-acetyl methyl of GlcNAc.

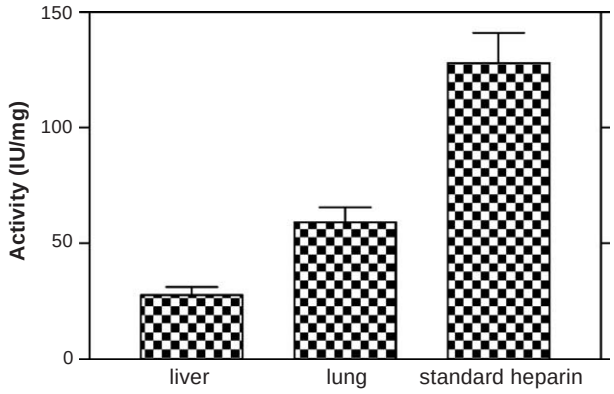

Fig. 6. The anticoagulant activity of camel liver and lung HS are expressed in units of anti-factor Xa activity and compared to pharmaceutical porcine intestinal heparin. Error bar is mean ± S.E.M. of at least 5 determinations.

found in porcine intestinal heparin (not shown), suggesting that these samples more closely resemble an HS than a heparin. Peaks **3**, **6**, **7** and **8** in the NMR spectra are relatively more prominent in camel lung HS than that of camel liver HS, suggesting that lung HS contained a relatively higher amount of glucuronic acid. The higher intensity of peak **9** also suggests that GlcNS is in greater abundance in camel lung than in camel liver HS, consistent with the results of the disaccharide analysis. It is also apparent that peak **1**, corresponding to GlcNS (H-1) and IdoA2S (H-1), is relatively higher in camel lung HS than in camel liver HS, confirming the higher level of 2-*O*-sulfo and *N*-sulfo groups in camel lung HS, consistent with its heparin-like character. Again, the disaccharide analysis is in accord with the results of the NMR analysis.

Heparin/HS chains have markedly heterogeneous structures in which distinct patterns of sulfation determine the binding specificity for ligand proteins (Capila and Linhardt, 2002; Linhardt, 2003). This "fine structure" of heparin/HS results from the differential introduction of sulfo groups at the *N*-, 2-*O*-, 6-*O*-, and 3-*O*-positions of the sugar chain during biosynthesis (Esko and Selleck, 2002). Recent biochemical, histochemical, and genetic studies have demonstrated that different fine structures mediate distinct molecular recognition events to regulate a variety of cellular functions (Nakato and Kimata, 2002; Capila and Linhardt, 2002). The anticoagulant activity of heparin and HS are related to the presence of a specific pentasaccharide sequence containing a rare 3-*O*-sulfo group (Linhardt, 2003). Unfortunately, disaccharide analysis fails to detect this sequence due to the inability of the heparin lyases to completely cut through all of the linkages to the uronic acids comprising this pentasaccharide (Yu et al., 2000). Thus, an anti-factor Xa amidolytic assay capable of detecting this pentasaccharide sequence was utilized to evaluate both camel liver and camel lung HS. Camel lung HS displayed a relatively higher anti-factor Xa activity than camel liver HS (Fig. 6). While the anti-factor Xa activity of camel lung HS was only 50% that of porcine intestinal heparin, its specific activity is considerably higher than most HS samples examined from various species and tissues. This result suggests that a more purified GAG preparation from camel lung might have potential clinical applications as an anticoagulant.

Normally, camel liver represents a very good model of more abundant fibrous tissue (Lalla and Drommer, 1997). The structure of HS from such a fibrous organ might address some questions on the relation between fibrous tissue procollagen and the HS structure. A link between transforming growth factor and PGs in liver fibrogenesis has previously been suggested (Kovalszky et al., 1988). Liver is a very active metabolic organ and generally has heparin/HS with a lower level of sulfation than intestinal tissues. Our findings are consistent with these results. Interestingly, camel liver HS has both less trisulfated (ΔUA2S–GlcNS6S) and unsulfated (ΔUA–GlcNAc) disaccharides than human and porcine liver HS. Thus, camel liver HS was remarkably similar to camel intestinal HS (Warda et al., 2003). The high percentage of intermediate and undersulfated disaccharides and low percentage of unsulfated or highly sulfated disaccharides in camel liver HS makes it fall between porcine liver HS and human liver HS in its degree of sulfation. The unusual sulfation pattern of camel liver HS is most likely related to its biosynthesis and may be responsible for differences in liver function in the camel (Abdel-Fattah et al., 1999). Camel lung HS also shows an interesting disaccharide analysis, intermediate between porcine intestinal heparin and the heparan sulfates examined (Table 1). From disaccharide analysis, data are unclear whether camel lung GAG is a highly sulfated HS, a mixture of HS and heparin or an undersulfated heparin.

In conclusion, this study demonstrates, for the first time, the structure of HS from the liver and lung of the one-humped camel. There are some unique differences in the disaccharide analysis of HS from camel liver compared to that of human and porcine liver. Camel lung HS has disaccharide composition more similar to heparin than HS and about 50% of heparin's anticoagulant actively as determined by anti-factor Xa assay. These results suggest the potential utility of camel lung GAG as a clinical anticoagulant, although further purification characterization, and pharmacological evaluation will be required. The disaccharide analysis of both lung and liver HS require further investigation to investigate the relation between the structure of these GAGs and the metabolism of this poorly studied animal.

References

Abdel-Fattah, M., Amer, H., Ghoneim, M.A., Warda, M., Megahed, Y., 1999. Response of one-humped camel (*Camelus dromedarius*) to intravenous glucagon injection and to infusion of glucose and volatile fatty acids, and the kinetics of glucagon disappearance from the blood. Zentralbl. Veterinarmed., Reihe A 46, 473–481.

Barth, H., Schaefer, C., Adam, M.I., Zhang, F., Linhardt, R.J., Della, E., von Weizsacker, F., Blum, H.E., Baumert, T.F., 2003. Cellular binding of hepatitis C virus envelop glycoprotein E2 requires cell surface heparan sulfate. J. Biol. Chem. 278, 41003–41012.

Bazin, H.G., Marques, M.A., Owens, A.P., Linhardt, R.J., Crutcher, K.A., 2002. Inhibition of apolipoprotein E-related neurotoxicity by glycosaminoglycans and their oligosaccharides. Biochemistry 41, 8203–8211.

Bitter, T., Muir, H.M., 1962. A modified uronic acid carbazole reaction. Anal. Biochem. 4, 330–334.

Bocksch, L., Stephens, T., Lucas, A., Singh, B., 2001. Apolipoprotein E: possible therapeutic target for atherosclerosis. Curr. Drug Targets Cardiovasc. Haematol. Disord. 1, 93–106.

Capila, I., Linhardt, R.J., 2002. Heparin–protein interactions. Angew. Chem., Int. Ed. Engl. 41, 390–412.

Cesaretti, M., Luppi, E., Maccari, F., Volpi, N., 2004. Isolation and characterization of a heparin with high anticoagulant activity from the clam *Tapes phylippinarum*: evidence for the presence of a high content of antithrombin III binding site. Glycobiology 14, 1275–1284.

Chen, Y., Maguire, T., Hileman, R.E., Fromm, J.R., Esko, J.D., Linhardt, R.J., Marks, R.M., 1997. Dengue virus infectivity depends on envelope protein binding to target cell heparan sulfate. Nat. Med. 3, 866–871.

Dittmann, J., Keller, C., Harisch, G., 1998. Inhibition of adenylate cyclase of rat hepatic membranes by glycosaminoglycans. Life Sci. 63, 2199–2208.

Dong, J., Peters-Libeu, C.A., Weisgraber, K.H., Segelke, B.W., Rupp, B., Capila, I., Hernáiz, M.J., LeBrun, L.A., Linhardt, R.J., 2001. Interaction of the N-terminal domain of apolipoprotein E4 with heparin. Biochemistry 40, 2826–2834.

Dumoulin, M., Conrath, K., Van Meirhaeghe, A., Meersman, F., Heremans, K., Frenken, L.G., Muyldermans, S., Wyns, L., Matagne, A., 2002. Single-domain antibody fragments with high conformational stability. Protein Sci. 11, 500–515.

Edens, R.E., Al-Hakim, A., Weiler, J.M., Rethwisch, D.G., Fareed, J., Linhardt, R.J., 1992. Gradient polyacrylamide gel electrophoresis for determination of the molecular weights of heparin preparations and low-molecular-weight heparin derivatives. J. Pharm. Sci. 81, 823–827.

Esko, J.D., Selleck, S.B., 2002. Order out of chaos: assembly of ligand binding sites in heparan sulfate. Annu. Rev. Biochem. 71, 435–471.

Gomes, P.B., Dietrich, C.P., 1982. Distribution of heparin and other sulfated glycosaminoglycans in vertebrates. Comp. Biochem. Physiol. B 73, 857–863.

Grant, A.C., Linhardt, R.J., Fitzgerald, G., Park, J.J., Langer, R., 1984. Metachromatic activity of heparin and heparin fragments. Anal. Biochem. 17, 25–32.

Griffin, C.C., Linhardt, R.J., Van Gorp, C.L., Toida, T., Hileman, R.E., Schubert, R.L., Brown, S.E., 1995. Isolation and characterization of heparan sulfate from crude porcine intestinal mucosal peptidoglycan heparin. Carbohydr. Res. 276, 183–197.

Hardingham, T.E., Fosang, A.J., 1992. Proteoglycans: many forms and many functions. FASEB J. 6, 861–870.

Ibrahimi, O.A., Yeh, B.K., Eliseenkova, A.V., Zhang, F., Olsen, S.K., Igarashi, M., Aaronson, S.A., Linhardt, R.J., Mohammadi, M., 2005. Analysis of mutations in FGF and a pathogenic mutation in FGFR provide direct evidence in support of the two-end model for FGFR dimerization. Mol. Cell. Biol. 25, 671–684.

Jurgens, K.D., Pietschmann, M., Yamaguchi, K., Kleinschmidt, T., 1988. Oxygen binding properties, capillary densities and heart weights in high altitude camelids. J. Comp. Physiol. B 158, 469–477.

Kovalszky, I., Nagy, P., Szende, B., Lapis, K., Szalay, F., Jeney, A., Schaff, Z., 1988. Experimental and human liver fibrogenesis. Scand. J. Gastroenterol. 228, 51–55.

Lalla, S., Drommer, W., 1997. Observations on the fine structure of the liver in the camel (*Camelus dromedarius*). Anat. Histol. Embryol. 26, 271–275.

Linhardt, R.J., 2003. Perspective: 2003 Claude S. Hudson Award address in carbohydrate chemistry. Heparin: structure and activity. J. Med. Chem. 46, 2551–2554.

Linhardt, R.J., Toida, T., 2004. Role of glycosaminoglycans in cellular communication. Accounts Chem. Res. 37, 431–438.

Mackenstedt, U., Brockelman, C.R., Mehlhorn, H., Raether, W., 1989. Comparative morphology of human and animal malaria parasites: I. Host–parasite interface. Parasitol. Res. 75, 528–535.

Medeiros, G.F., Mendes, A., Castro, R.A., Bau, E.C., Nader, H.B., Dietrich, C.P., 2000. Distribution of sulfated glycosaminoglycans in the animal kingdom: widespread occurrence of heparin-like compounds in invertebrates. Biochim. Biophys. Acta 1475, 287–294.

Nakato, H., Kimata, K., 2002. Heparan sulfate fine structure and specificity of proteoglycan functions. Biochim. Biophys. Acta 1573, 312–318.

Nazifi, S., Gheisari, H.R., Poorkabir, M.A, Saadatfar, S., 2000. Serum lipids and lipoproteins in clinically healthy male camels (*Camelus dromedarius*). Vet. Res. Commun. 24, 527–531.

Nobuo, N., 2003. Metabolism of heparan sulfate proteoglycans in *Drosophila* cell lines. Kokubyo Gakkai Zasshi. J. Stomatological Soc. 70, 40–45.

Pervin, A., Gallo, C., Jandik, K.A., Han, X., Linhardt, R.J., 1995. Preparation and structural characterization of large heparin-derived oligosaccharides. Glycobiology 5, 83–95.

Peterson, F.C., Elgin, E.S., Nelson, T.J., Zhang, F., Hoeger, T.J., Linhardt, R.J., Volkman, B.F., 2004. Identification and characterization of a glycosaminoglycan recognition element of the C chemokine lymphotactin. J. Biol. Chem. 279, 12598–12604.

Rathore, D., McCutchan, T.F., Hernáiz, M.J., LeBrun, L.A., Lang, S.C., Linhardt, R.J., 2001. Direct measurement of the interaction of glycosaminoglycans and a heparin decasaccharide with malaria circumsporozoite protein. Biochemistry 40, 11518–11524.

Schonberger, L.B., 1998. New variant Creutzfeldt–Jakob disease and bovine-spongiform encephalopathy. Infect. Dis. Clin. North Am. 12, 111–121.

Teien, A.N., Lei, M., 1977. Evaluation of an amidolytic heparin assay method: increased sensitivity by adding purified antithrombin III. Thromb. Res. 10, 399–410.

Teien, A.N., Lie, M., Abildgaard, U., 1976. Assay of heparin in plasma using a chromogenic substrate. Thromb. Res. 8, 413–416.

Thanawiroon, C., Linhardt, R.J., 2003. Separation of complex mixture of heparin derived oligosaccharides using reversed-phase high performance liquid chromatography. J. Chromatogr. A 1014, 214–223.

Toida, T., Yoshida, H., Toyoda, H., Koshiishi, I., Imanari, T., Hileman, R.E., Froman, J.R., Linhardt, R.J., 1997. Structural differences and the presence of unsubstituted amino groups in heparin sulphates from different tissues and species. Biochem. J. 322, 499–506.

Vongchan, P., Warda, M., Toyoda, H., Toida, T., Marks, M., Linhardt, R.J., 2005. Structural characterization of human liver heparan sulfate. Biochim. Biophys. Acta 1721, 1–8.

Warda, M., Zeisig, R., 2000. Phospholipid- and fatty acid-composition in the erythrocyte membrane of the one-humped camel [*Camelus dromedarius*] and its influence on vesicle properties prepared from these lipids. Dtsch. Tierarztl. Wochenschr. 107, 368–373.

Warda, M., Gouda, E.M., Toida, T., Chi, L., Linhardt, R.J., 2003. Isolation and characterization of raw heparin from dromedary intestine: evaluation of a new source of pharmaceutical heparin. Comp. Biochem. Physiol. B 136, 357–365.

Warda, M., Gouda, E.M., El-Behairy, A.M., Mousa, S.Z., submitted for publication. Conserved and non-conserved loci of glucagon gene in old world ruminating ungulates: a comparative study. Z. Naturforsch C.

Yu, G., LeBrun, L., Gunay, N.S., Hoppensteadt, D., Walenga, J., Fareed, J., Linhardt, R.J., 2000. Heparinase I acts on a synthetic heparin pentasaccharide corresponding to the antithrombin III binding site. Thromb. Res. 100, 549–556.

Yu, H., Edens, R.E., Linhardt, R.J., 2005. Regulation activity of heparin in complement system in the Chemistry and Biology of Heparin and Heparan Sulfate, Elsevier Ltd., Oxford. In: Garg, H.G., Linhart, R.J., Hales, C.A. (Eds.), pp. 315–345 (Chapter II).